Accuracy of chaos synchronization in Nd:YVO_4 microchip lasers

A. Uchida, T. Ogawa, M. Shinozuka, and F. Kannari
Department of Electrical Engineering, Keio University, 3-14-1 Hiyoshi, Kohoku-ku, Yokohama 223-8522, Japan
(Received 1 December 1999)

Synchronization of chaotic oscillations generated in two Nd:YVO_4 microchip lasers is experimentally and numerically demonstrated with master-slave coupling schemes. The synchronization performance under some parameter mismatch between the two lasers is quantitatively characterized. Synchronization is always achieved when the lasing frequency of the slave laser is matched to that of the master laser through injection locking. Accurate synchronization of chaos at an average intensity error of less than 2% is attained and maintained for tens of hours. The modulation parameters of the two lasers do not need to be matched for synchronization when the injection power is at a sufficiently high level, because chaos synchronization is based on its injection-locking performance. For accurate synchronization in multimode lasers, the power distribution among longitudinal modes needs to be matched.

PACS number(s): 05.45.Xt, 42.65.Sf, 05.45.Vx, 05.45.Gg

I. INTRODUCTION

Synchronization of chaos has recently attracted great interest because of its potential applications in secure communications [1,2]. Optical chaos generated in lasers, in particular, is expected to be useful for optical secure communications. Recently, optical encryption systems using laser chaos were experimentally demonstrated [3–5], where synchronization of laser chaos is a key technology to generate an identical chaotic wave form in both a transmitter and a receiver for signal decoding. Synchronization of chaos in lasers has been intensively investigated with numerical models [6–26] and in experiments [27–38] for various laser systems. However, no one has reported the physical mechanism of chaos synchronization in lasers, so far. Therefore, experimental conditions for achieving chaos synchronization are still not well understood. Chaos synchronization in lasers can be categorized into two types: the master-slave type (unidirectional coupling of the laser field) and the mutually coupled type [6]. In this paper, we discuss chaos synchronization only in the master-slave type, which is well suited for secure communication applications to connect distantly separated chaotic lasers and to maintain the original chaotic carriers.

The concept of chaos synchronization was first reported by Pecora and Carroll [1]. A chaotic system is divided into two subsystems, the driving and response systems. The response system (master) and another newly created response system (slave) are synchronized by applying a signal from the driving subsystem. Synchronization can be achieved when all the conditional Lyapunov exponents in the response systems are negative. In fact, this method is not suited for synchronization in lasers, which cannot be completely divided into two subsystems. For more practical techniques, a continuous control method has been proposed [39,40], where the difference between two chaotic signals ($\Delta x = x_{\mathrm{master}} - x_{\mathrm{slave}}$) is fed back to a slave system. For the differential signal to be kept to zero under perfect synchronization ($\Delta x = 0$), all the system parameters have to be identical. Thus, a synchronous solution always exists in such systems. When the two chaotic signals tend to be slightly different, negative feedback can control the system at the manifold of $x_{\mathrm{master}} = x_{\mathrm{slave}}$. Some numerical studies on chaos synchronization in lasers using this method have been reported [8–10]. However, since coherent detection of the difference between two laser fields is complicated in experiments, the laser field in the master laser is directly injected into the slave laser for synchronization [6,11–26]. In this case, a perfect synchronous solution can exist when the injection power ratio and/or photon lifetime in the laser cavity are carefully adjusted in both the master and slave lasers [11,12,17]. Therefore, the optical injection method for chaos synchronization in lasers appears to be equivalent to the continuous control method.

These synchronization mechanisms cannot be adopted when parameter mismatch exists between chaotic systems. There is no synchronous solution. Some numerical studies on chaos synchronization in lasers with parameter mismatch have been reported [6,8,12–18]. They found that the accuracy of synchronization is reduced as the parameter mismatch increases. The most important condition for achieving synchronization in lasers is matching carrier frequencies between the two lasers. Note that lasing frequencies are very much larger than chaotic oscillation frequencies by a factor of 10^5–10^9. We denote the amplitude of the electrical field $\dot{E}(t) = \dot{E}_0(t)\exp(i\omega_0 t)$. The slowly varying envelope approximation allows us to eliminate the term $\exp(i\omega_0 t)$ and we can consider only the dynamics of the slowly varying electrical field envelope $\dot{E}_0(t)$. In the presence of detuning between the lasing frequencies $\Delta\omega_0 = \omega_{0,\mathrm{master}} - \omega_{0,\mathrm{slave}}$, the optical field injected into the slave laser can be described as $\dot{E}_0(t)\exp(i\Delta\omega_0 t)$. Thus, a synchronous solution does not exist at $\Delta\omega_0 \neq 0$. In this case, the optical injection method for synchronization is not equivalent to the continuous control method.

Although there are a few reports about loss of synchronization via detuning of lasing frequencies [12,13,15,16], a constant detuning was always assumed in these studies. When the master laser is injected into the slave laser for synchronization, injection locking is achieved and the lasing

frequency of the slave laser is pulled to that of the master laser, if natural lasing frequencies of both lasers are within a certain locking range [41]. This injection-locking mechanism was not taken into account in previous reports. Since detuning of lasing frequencies can be eliminated as a result of proper injection locking, a synchronous solution exists in actual laser systems. When the injected master laser is resonant in the slave laser cavity ($\omega_{0,\mathrm{master}}=\omega_{0,\mathrm{slave}}$), the slowly varying envelope component within a certain bandwidth can be regenerated in the slave laser [$E_{0,\mathrm{master}}(t)=E_{0,\mathrm{slave}}(t)$]. Therefore, it is not adequate to discuss the chaos synchronization between two chaotic laser systems from the same viewpoint as electric circuits, since injection locking in the laser cavity is a mechanism that is not used in electric circuits.

Some experimental studies have revealed that chaos synchronization is achieved when the lasing frequencies are locked to each other [30,33,34,38]. Here, ''chaos synchronization'' in experiments is defined as the reproduction of identical chaotic wave forms in two separate lasers, including regeneration of chaos by injection locking. However, these references did not mention whether injection locking is necessary and/or sufficient for synchronization. Therefore, it is important to clarify the physical mechanism of chaos synchronization in lasers and the requirement of injection locking for synchronization.

In this paper, we investigate the physical mechanism of experimental chaos synchronization in lasers with a master-slave optical coupling type. We experimentally and numerically demonstrate synchronization of chaos in a master-slave type system with two separate diode-pumped Nd:YVO_4 microchip solid-state lasers, in which chaotic wave forms can easily be generated by modulation of pumping [38] or using frequency-shifted feedback light [42–45]. We quantitatively estimate the accuracy of chaos synchronization from our experimentally obtained temporal wave forms by use of the variance of correlation plots between the two laser intensities. Degradation of the accuracy of synchronization is investigated in detail when the parameters in the two lasers are mismatched. We also clarify the different characteristics of synchronization of single-mode and multimode lasers.

This paper is organized as follows. Section II describes our experimental setup of chaos synchronization and the procedure for injection locking. In Sec. III, we experimentally demonstrate synchronization of chaos and estimate the requirements for parameter matching between two lasers to achieve accurate synchronization. We also discuss the principle of synchronization. The characteristics of synchronization in single-mode and two-mode lasers are compared. In Sec. IV, we numerically investigate synchronization of chaos in microchip lasers. Our numerical results agree well with our experimental results. Finally, we draw conclusions from our results in Sec. V.

II. EXPERIMENTAL SETUP

Figure 1 shows our experimental setup for chaos synchronization. We used two Nd:YVO_4 microchip crystals (1.1 atomic % doped; Fujian Crystals Inc.), which were obtained from the same crystal rod. Both ends of the 1-mm-long crystals were coated in the same process with dielectric mirrors

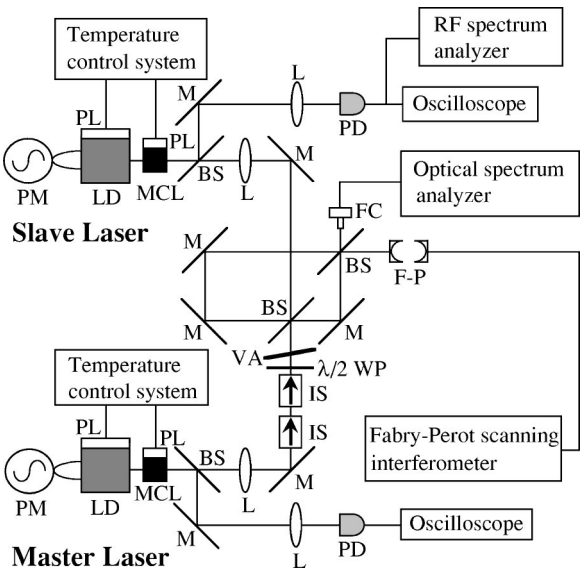

FIG. 1. Experimental setup for chaos synchronization in two Nd:YVO_4 microchip lasers with pump modulation in master-slave type I (MS-1): BS's, beam splitters; L's, lenses; M's, mirrors; VA, variable attenuator (neutral density filter); LD's, laser diodes; MCL's, Nd:YVO_4 microchip lasers; PL's, Peltier devices; IS's, optical isolators; PD's, photodiodes; FC, fiber coupler; PM's, pump modulations; λ/2 WP, λ/2 wave plate; F-P, Fabry-Pérot étalon.

($R_1=99.8\%$, $R_2=99.1\%$) for a lasing wavelength of $\lambda=1064$ nm. The free spectral range of the laser cavity was 79 GHz. Each crystal was pumped by a fiber coupled laser diode (Opt Power Co., OPC-A001-809-FC/100, $\lambda=809$ nm) with two focusing lenses. The laser oscillated with 1–3 longitudinal modes depending on the pumping power. The temperatures of the microchip crystals and the laser diodes were controlled with thermoelectric coolers (resolution of 0.01 K) for fine tuning of the laser frequencies.

Chaotic outputs in microchip lasers are easily obtained by modulating the pumping (called pump modulation [38]) or by injecting the frequency-shifted feedback light (called loss modulation) causing beat oscillations [42–45], both on the order of the sustained relaxation oscillation frequencies (a few MHz). During the experiments in this paper, we used pump modulation. The injection current of a laser diode used for pumping was sinusoidally modulated.

As shown in Fig. 1, a fraction of the master laser output was injected into the slave laser cavity for chaos synchronization. Two optical isolators (Electro-Optics Technology Inc., 1845-2) and a λ/2 wave plate were used to achieve one-way coupling from the master to the slave lasers (isolation of −60 dB). Chaotic temporal wave forms were detected by photodiodes (Hamamatsu Photonics Inc., G3476-03) and digital oscilloscopes (Sony Tektronix, TDS410). The optical frequencies of the lasers were measured by an optical spectrum analyzer (Advantest, Q8381A) and a Fabry-Pérot scanning interferometer (TEC-Optics, SA-7.5) with a free spectral range of 7.5 GHz and a finesse of 250.

Achievement of synchronization of chaos is highly dependent on the injection-locking performance of the slave oscillator. The optical frequencies of two individual lasers can be perfectly matched by injection locking when the frequency

difference is set within the injection-locking range. The injection-locking range $\Delta\nu_{\mathrm{lock}}$ is described by [41]

$$\Delta\nu_{\mathrm{lock}} \leqq \frac{\nu_s}{Q_s}\sqrt{\frac{P_m}{P_s}}, \tag{2.1}$$

where ν_s is the optical frequency in the slave laser, Q_s is the Q value of the slave laser cavity, and $P_{m,s}$ are the injected power from the master and the intracavity power of the slave laser, respectively. Therefore, the injection-locking range is dependent on the injection power of the master laser output. In our experiments, the injection-locking range was approximately 200 MHz.

The optical frequencies of Nd:YVO_4 microchip lasers can be tuned linearly as a function of the temperature of the crystals at 1.6 GHz/K [46]. The temperature of the crystal in the master laser was kept constant. The temperature of the slave laser crystal was changed so that the difference of the two optical frequencies was within the injection-locking range. The optical frequencies were adjusted from a low resolution to a high resolution by monitoring the spectra with the optical spectrum analyzer (resolution of 30 GHz), the Fabry-Pérot scanning interferometer (resolution of 30 MHz), and the radio frequency spectrum analyzer (resolution of 1 kHz). Then a frequency beat between the two lasers was observed on the radio frequency spectrum analyzer. When the beat frequency was settled within the injection-locking range ($\sim$200 MHz) with more accurate temperature control, the beat frequency disappeared and the two laser frequencies were perfectly matched. In our experiments, the final temperatures of the microchip crystals were set to 315.00 K and 287.39 K for the master and slave lasers, respectively. The output powers of the microchip lasers were set to 0.02 mW and 0.82 mW (measured in front of the slave laser cavity) for the master and slave lasers, respectively.

III. EXPERIMENTAL RESULTS AND DISCUSSION

A. Chaos synchronization in single-mode lasers

To investigate the operating conditions of the slave laser for chaos synchronization, we categorized master-slave synchronization schemes into two types [6]. A master-slave type I (MS-1) consists of a chaotic master laser and a chaotic slave laser with a positive Lyapunov exponent. A master-slave type II (MS-2) is composed of a chaotic master laser and a nonchaotic slave laser with a negative Lyapunov exponent.

First, we tried to synchronize chaos using MS-1. Both lasers oscillated with only one longitudinal mode. The injection currents of the laser diodes in the two lasers were adjusted so that the sustained relaxation oscillation frequencies in the two lasers were matched (1.38 MHz). When pump modulations were applied to both the microchip lasers near the sustained relaxation oscillation frequency (for example, a modulation frequency of 1.34 MHz with a modulation depth of 18%), individual chaotic pulsations were obtained. Figures 2(a) and 2(b) show the chaotic temporal wave forms and the distribution of 5000 data points in a correlation plot between the two laser outputs. There is no correlation at all between the chaotic pulsations in the two lasers. When a fraction of the master laser output was injected into the slave laser cavity within the injection-locking range described before, the chaotic oscillations were synchronized as shown in Fig. 2(c). The linear correlation between the two laser outputs shown in Fig. 2(d), in contrast with Fig. 2(b), exhibits the synchronization. This synchronization can be maintained for tens of hours as long as the injection locking of the two laser frequencies is achieved.

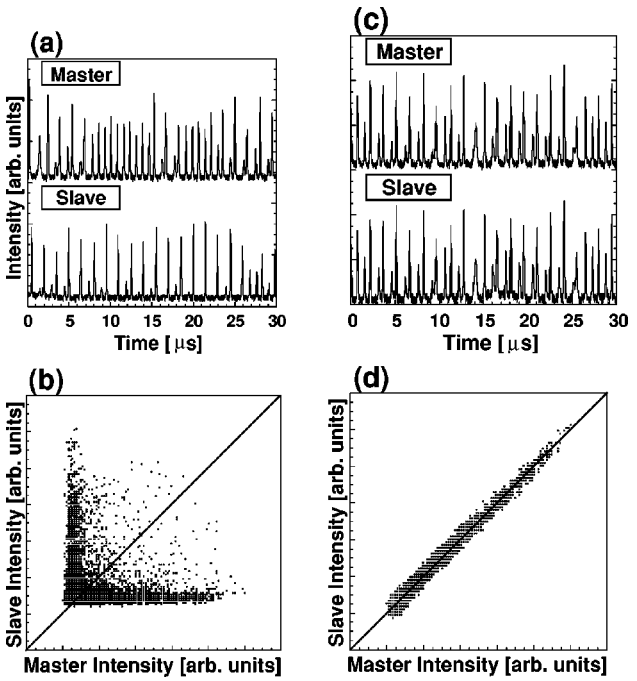

FIG. 2. Experimentally obtained chaotic temporal wave forms and correlation plots for the two laser outputs: (a),(b) without synchronization and (c),(d) with synchronization in MS-1 with single-mode oscillations.

Next, we tried synchronization of chaos with the MS-2 coupling type. The temporal wave forms in the slave laser exhibit a sustained relaxation oscillation as shown in Figs. 3(a) and 3(b). When injection locking was achieved between the two laser frequencies, the chaotic output in the master laser was reproduced in the slave laser [Fig. 3(c)]. The correlation plot of Fig. 3(d) shows accurate reproduction of the chaos as good as that achieved in MS-1 shown in Fig. 2(d).

To evaluate the quantitative accuracy of chaos synchronization, the variance σ^2 of the normalized correlation plot from a best-fit linear relation is used, which is defined as [27]

$$\sigma^2 = \frac{1}{N}\sum_{i}^{N}(I_{m,i} - I_{s,i})^2, \tag{3.1}$$

where N is the total number of sampling points of the temporal wave forms (15 000 points) and $I_{m,i}$ and $I_{s,i}$ are the normalized intensities of the master and slave lasers at the ith sampling point. A smaller variance σ^2 implies higher accuracy of chaos synchronization. The variances of the MS-1 [Fig. 2(d)] and MS-2 [Fig. 3(d)] coupling schemes are $\sigma^2 = 0.000\,56$ and $0.000\,55$, respectively, that is, we found that the variances of MS-1 and MS-2 are very similar. A very accurate synchronization with an average error of 2% ($\sigma = 0.024$) was obtained.

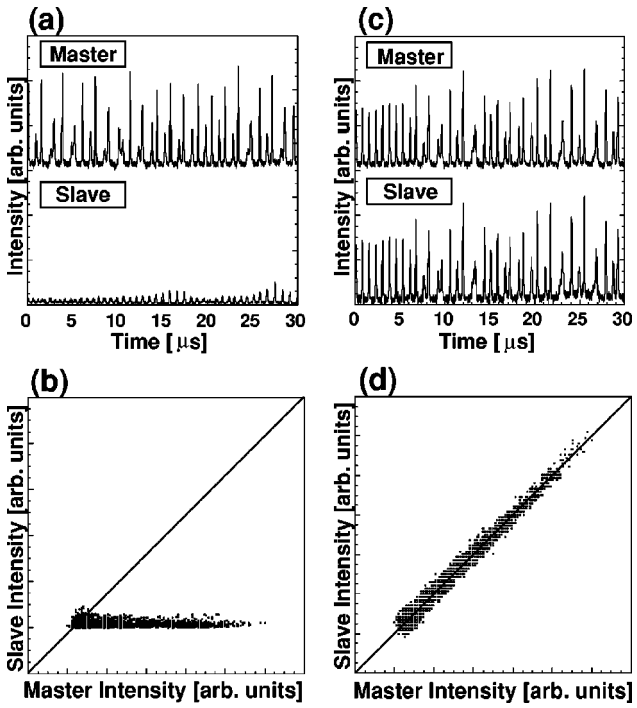

FIG. 3. Experimentally obtained chaotic temporal wave forms and correlation plots for the two laser outputs: (a),(b) without synchronization and (c),(d) with synchronization in MS-2 (nonchaotic slave laser) with single-mode oscillations.

B. Quantitative characterization of chaos synchronization

We quantitatively investigated the characteristics of chaos synchronization performance when various laser parameters are changed in the two lasers. First, we evaluated the synchronization performance when the injection-locking performance was slightly altered. In the following description, the injection-locking performance was separately examined under nonchaotic conditions without the pump modulation. Figure 4(a) shows the variances of the correlation plots as a function of injected power from the master to the slave lasers. The injection power was altered with a variable attenuator (a neutral density filter). We found that accuracy of synchronization is always quite high at any injection power higher than the threshold. Above the threshold, relatively constant variances are maintained as the injection power increases. Therefore, the synchronization range coincides with the injection-locking range. These results are different from that in laser diodes [5,14,29], where an optimum coupling coefficient exists to achieve accurate synchronization. We speculate that the difference comes from stability of the injection-locking performance. Injection locking in laser diodes itself induces a variety of nonlinear dynamics such as chaos, period-doubling bifurcation, and multiwave mixing [47], due to the existence of the linewidth enhancement factor (α parameter) in diodes, whereas injection locking in microchip lasers is always stable if the injection-locking bandwidth is much larger than the sustained relaxation oscillation frequencies ($\sim$a few MHz) [48].

Next, the temperature of the slave crystals was slightly shifted from the perfect injection-locking point, which causes detuning. A beat oscillation was observed on the spectrum analyzer. We investigated the synchronization range under oscillation frequency detuning. Figure 4(b) shows the variances of the correlation plots as a function of the beat frequency at two constant injection powers. Low and constant variances are maintained within the injection-locking range. Therefore, again, the synchronization range coincides with the injection-locking range.

We also investigated accuracy of synchronization when one of the parameters for chaos generation is mismatched between the two lasers. First, the amplitude or the frequency of the pump modulation in the slave laser was slightly shifted from that in the master laser. Figure 5 shows variances as functions of the amplitude and frequency of the pump modulation in the slave laser under weak and strong injection powers. A modulation amplitude of 10% at the frequency of 1.34 MHz was maintained for the master laser (the downward arrows in Fig. 5). With weak injection power (solid circles, transmittance of a coupling filter of 0.09%), the variance increases as the modulation amplitude increases. It is worth noting that matching of the modulation amplitude is not required to achieve accurate synchronization. The best synchronization is achieved without modulation in the slave laser, which corresponds to the MS-2 coupling type. On the other hand, a low variance is always maintained with strong injection power (open circles, transmittance of a coupling filter of 100%) even if the modulation amplitude increases. These results imply that intense injection of the master laser can suppress the original dynamics in the slave laser, and the accuracy of synchronization is independent of the mismatch of the pump modulation between the master and slave lasers. With weak injection power, accurate synchronization can be realized only when the pump modulation is weak enough in the slave laser to allow the injected master laser oscillation to suppress the slave laser chaos. Therefore, generation of chaos in the slave laser is undesirable.

Figure 5(b) shows that the variance increases at modulation frequencies less than 1 MHz for weak injection power, because the synchronized temporal wave forms periodically change at a low frequency corresponding to the pump modulation of the slave laser. This is a unique feature observed only for pump modulation. With strong injection locking, the variance is kept low. Therefore, perfect matching in pump modulation frequency is not required if the injection power is high enough.

According to the results of Fig. 5, we speculate that the principle of synchronization of chaos in lasers is based on regeneration of the chaotic master laser in the slave cavity through injection locking. When the master chaos can suppress the original chaos in the slave laser, a duplicated chaotic oscillation is obtained from the slave laser. The original chaos in the slave laser only disturbs the perfect regeneration of the master chaos in the slave cavity. If the injected master laser power is strong enough, accurate synchronization is maintained even when the modulation parameters are significantly mismatched, because only the locking of optical frequencies is required. Since the best synchronization performance is always obtained when the pump modulation is not applied to the slave laser (MS-2), parameter matching is not required for synchronization of laser chaos, in contrast to the case in electrical circuits [2].

To confirm our interpretation, we experimentally investigated the performance of chaos synchronization for various

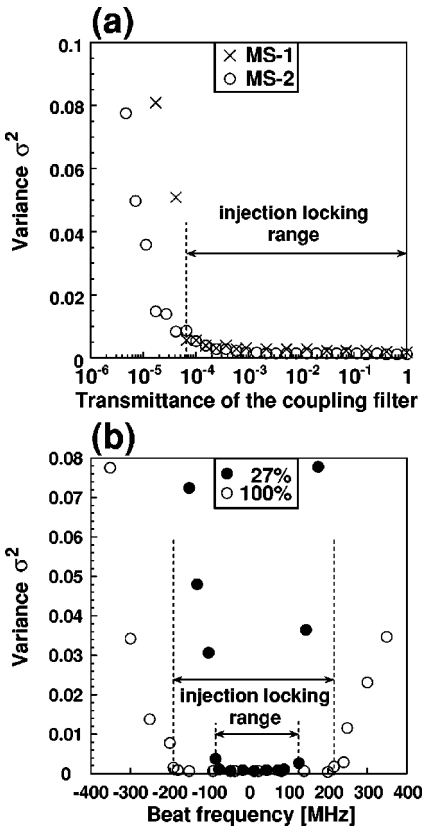

FIG. 4. Variances of the correlation plots as functions of (a) injected power and (b) beat frequency between the two optical frequencies. (a) Crosses, MS-1; circles, MS-2. (b) Solid circles, transmittance of a coupling filter of 27%; open circles, transmittance of a coupling filter of 100%. The arrows indicate injection-locking range.

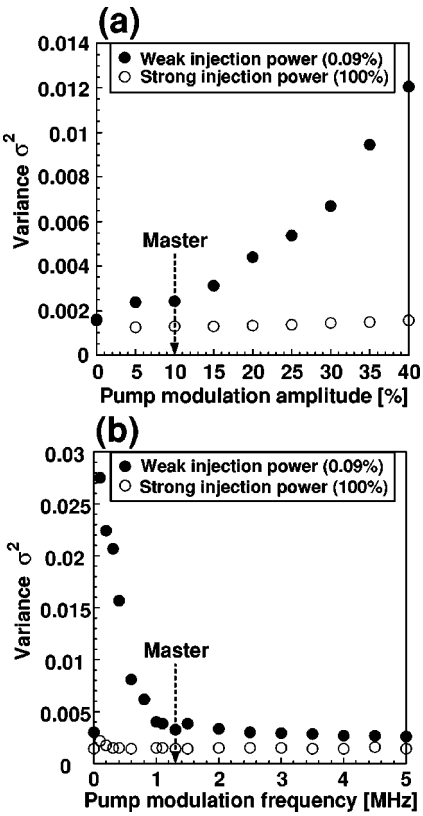

FIG. 5. Variances as functions of (a) amplitude and (b) frequency of the pump modulation in the slave laser. Solid circles, transmittance of a coupling filter of 0.09% (weak injection power); open circles, transmittance of a coupling filter of 100% (strong injection power). The downward arrows indicate parameter matching between the master and slave lasers.

parameter mismatch conditions using loss modulation. We used frequency-shifted feedback light generated by two series of acousto-optic modulators (AOM's), so that the beat frequency of the two modulators appears in feedback light, instead of the conventional method with a rotating paper sheet [42–45]. With this setup, the modulation frequency and amplitude can be controlled electrically with a high resolution of 0.1 kHz. Figure 6 shows variances as functions of amplitude and frequency of the loss modulation in the slave laser under different injection powers. The modulation amplitude (the amount of frequency-shifted feedback light) was changed with a variable attenuator. With weak injection power (solid circles, transmittance of injection power of 0.27%) in Fig. 6(a), the variance increases as the modulation amplitude increases. The modulation amplitude does not need to be matched in the two lasers, as we thought. With strong injection power (open circles, transmittance of injection power of 100%), the variance is always kept low. In Fig. 6(b), we used the two levels of feedback light power for loss modulation [the ratios of the injection power to the feedback light power are 1:6 (solid circles) and 1:0.4 (solid triangles)]. With strong feedback light for loss modulation (solid circles), the effect of loss modulation is enhanced and the variance dramatically decreases at the matched modulation frequency of 1.34 MHz. Thus, there is clear evidence of a parameter matching region for accurate synchronization. However, in terms of the level of accuracy, the variance obtained with no loss modulation is still lower. With strong injection power (open circles), the variance is kept low.

Next, we changed the pumping power of the two lasers. We set a strong injection power (transmittance of 100%) with the configuration of MS-1. Figure 7 shows variances as functions of pumping power of (a) the master and (b) the slave lasers under strong injection power. The number of longitudinal modes increases as the pumping power is increased as shown in Fig. 7. The laser in which we do not change the pumping power was set to oscillate with a single mode (the arrows in the figures). It is found that the variance is maintained at a constant level as long as both the lasers oscillate with a single mode. Around the oscillation threshold ($\leqslant 1.1$), the variance increases simply because there is less laser power. From these results, it is clear that the pumping power and the relaxation oscillation frequencies (proportional to the square root of the pumping power) do not need to be matched between the two lasers for accurate synchronization. It is important to match the number of longitudinal modes for synchronization, since one of the longitudinal modes cannot be locked between a single-mode and a two-mode laser. Therefore, achieving injection locking is more important for accurate synchronization than matching the modulation parameters and the pumping power.

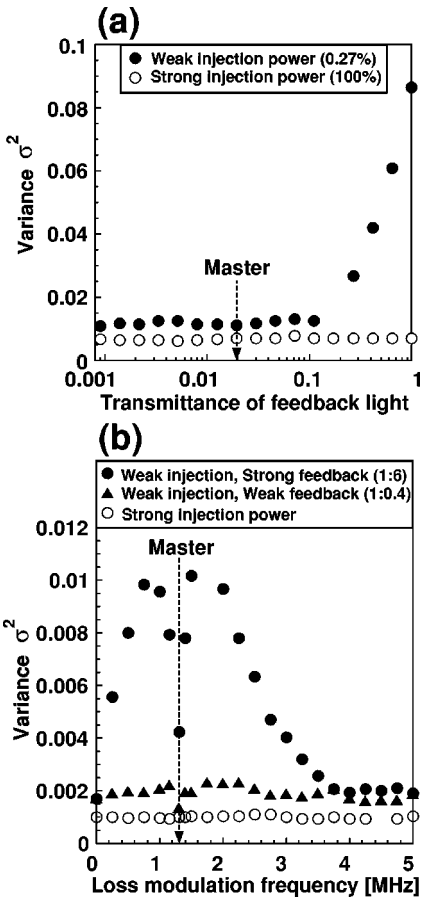

FIG. 6. Variances as functions of (a) amplitude and (b) frequency of loss modulation in the slave laser. Solid circles and triangles, transmittance of a coupling filter of 0.27% (weak injection power); open circles, transmittance of a coupling filter of 100% (strong injection power). The ratios of the injection power to the feedback light power are 1:6 (solid circles) and 1:0.4 (solid triangles). The downward arrows indicate parameter matching between the master and slave lasers.

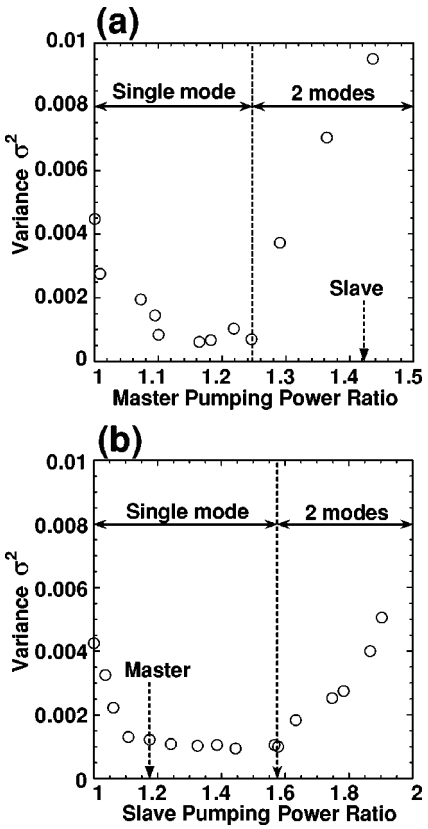

FIG. 7. Variances as functions of pumping power in (a) the master and (b) the slave lasers under strong injection power (transmittance of a coupling filter of 100%). The downward arrows indicate parameter matching between the master and slave lasers.

C. Chaos synchronization in two-mode lasers

For single-mode lasers, it is relatively easy to reproduce the chaotic wave forms of the master lasers by using unauthorized lasers without knowing the parameter values of the master laser because the accuracy of synchronization is independent of the parameter mismatch between two lasers under strong injection power. This is an issue when synchronization of chaos is applied to secure communications. Here, we tried to investigate synchronization of chaos in two-longitudinal-mode microchip lasers. Pump modulations (3.88 MHz, 8%) were applied to the master and slave lasers (MS-1) to generate chaos around the sustained relaxation oscillation frequencies ($f_{r1}=4.20$ MHz, $f_{r2}=1.84$ MHz). Figures 8(a) and 8(b) show individual chaotic wave forms and a correlation plot without injection locking. The shape of the chaotic oscillations is a continuous wavelike behavior, which is different from the pulselike behavior in single-mode lasers shown in Fig. 2, because at least one of the longitudinal modes always oscillates as a result of spatial hole burning of the population inversion in multimode lasers. When injection locking is achieved between the two lasers, synchronization of chaos is achieved as shown in Fig. 8(c). Linear correlation exhibiting highly accurate synchronization is obtained as shown in Fig. 8(d), where the variance is $\sigma^2=0.000\,29$ and the average intensity error is 1.7% ($\sigma=0.017$). Accurate synchronization is achieved in both MS-1 and MS-2 in two-mode lasers, and maintained for over tens of hours as in single-mode lasers.

Synchronization in multimode lasers requires locking all the corresponding longitudinal modes to each other between two lasers. When the temperature of the laser crystal is changed, the beat frequencies of the first and second modes are changed. Figure 9 shows the variances as a function of temperature of the microchip crystal in the slave laser. The arrows in this figure correspond to the injection-locking ranges for the first and second modes. When the frequency locking between one of the two modes is destroyed, the variance increases dramatically. Both modes should be locked for synchronization. In our experiments, the difference of the free spectral range (79 GHz) of the cavity between the master and slave lasers is only 0.05–0.20 GHz (depending on the temperature of the crystals), because the two microchip crystals were obtained from the same crystal rod and were fabricated in the same process. Therefore, injection locking of both modes can be achieved in these crystals (injection locking range of ~ 0.2 GHz). However, it is difficult to synchronize chaos between two multimode lasers that have greatly different free spectral ranges. Therefore, the condition for

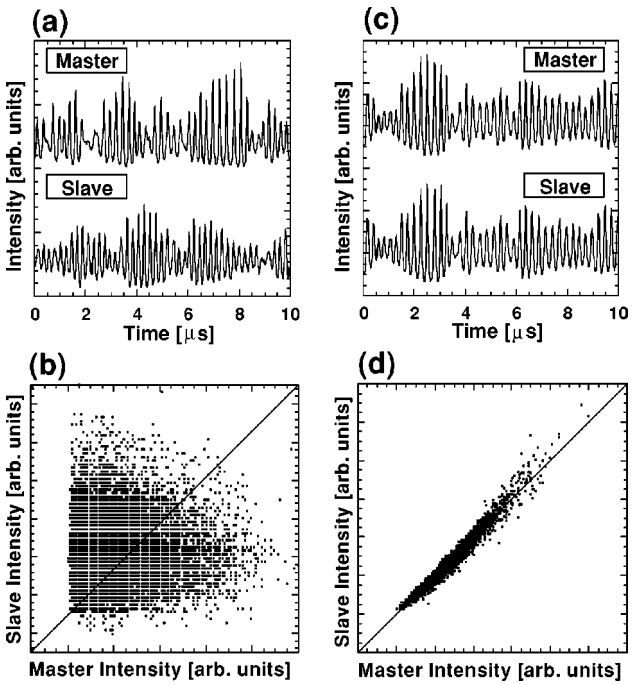

FIG. 8. Experimentally obtained chaotic temporal wave forms and correlation plots for the two laser outputs: (a),(b) without synchronization and (c),(d) with synchronization in MS-1 with two-longitudinal-mode oscillations.

synchronization in multimode lasers is more severe than that in single-mode lasers.

For two-mode lasers, accuracy of synchronization does not depend on the mismatch of the modulation parameters and the pumping power between the two lasers. However, it is important to match the power spectrum ratio of two longitudinal modes between the master and slave lasers for more accurate synchronization. Figure 10 shows optical spectra of the master and slave laser outputs after synchronization with two-mode oscillations, and the corresponding correlation plots. The power ratio of the longitudinal modes in the slave laser can be changed by controlling the temperature of the microchip crystal of the slave laser. Accurate synchronization is achieved when the power ratio between the first mode and the second mode in the slave laser approaches that of the master laser. Figure 11 shows characteristics of the variance as a function of the power spectrum ratio of the second mode to the first mode of the slave laser after synchronization. The arrow in the figure corresponds to the ratio of the second mode to the first mode of the master laser. This result implies that the amplification ratio of the first and second modes of the master laser should be the same in the slave cavity. The best resonant conditions of the first and second modes of the master laser are slightly different from those of the slave laser, if there is a difference in the free spectral ranges of the master and slave laser cavities. Thus, accurate synchronization in multimode lasers requires some parameter setting. This is a more severe condition to imitate the original chaos with other unauthorized lasers than that in single-mode laser systems. Therefore, chaotic wave

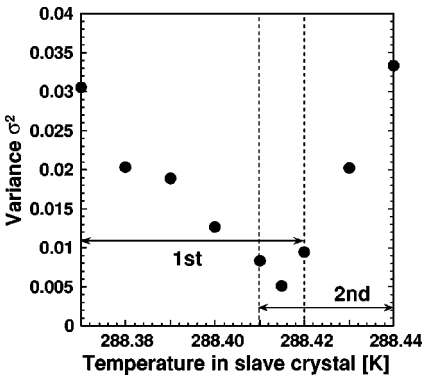

FIG. 9. Variances as a function of temperature of the microchip crystal in the slave laser. The injection-locking ranges for the first and second modes are indicated.

forms in multimode lasers are suitable for applications in secure communications.

We summarize the influence of parameter mismatch on accuracy of synchronization under strong injection power in Table I. The most important effect for synchronization of laser chaos is injection locking, which is the matching of optical frequencies ($\sim 10^{14}$ Hz) between the master and slave lasers. On the other hand, the slow envelope components such as the modulation frequency and the relaxation oscillation frequency ($\sim 10^{6}$ Hz) do not need to be matched under strong injection power, because the slow component in the slave laser is pulled into that of the master laser by injection locking. Therefore, we conclude that the principle of synchronization of chaos in lasers of the master-slave type is based on the regeneration of the chaotic master laser in the slave laser cavity by injection locking.

IV. NUMERICAL CALCULATIONS

A. Model

To confirm our experimental results, we numerically solved the dynamical model of two Nd:YVO_4 microchip lasers with pump modulation, which are optically coupled in MS-1. We used scaled Tang-Statz-deMars equations including spatial hole burning effects [43,45,49]. The rate equations under single-longitudinal-mode operation are as follows:

$$\frac{dn_{0,\mathrm{m}}}{dt} = w_{0,\mathrm{m}}[1 + w_{\mathrm{p,m}} \cos(2\pi\tau f_{\mathrm{p,m}} t + \Phi_{\mathrm{m}})] - n_{0,\mathrm{m}} - \left(n_{0,\mathrm{m}} - \frac{n_{1,\mathrm{m}}}{2}\right) E_{\mathrm{m}}^2, \tag{4.1}$$

$$\frac{dn_{1,\mathrm{m}}}{dt} = -n_{1,\mathrm{m}} + (n_{0,\mathrm{m}} - n_{1,\mathrm{m}}) E_{\mathrm{m}}^2, \tag{4.2}$$

$$\frac{dE_{\mathrm{m}}}{dt} = \frac{K_{\mathrm{m}}}{2}\left[\left(n_{0,\mathrm{m}} - \frac{n_{1,\mathrm{m}}}{2}\right) - 1\right] E_{\mathrm{m}}, \tag{4.3}$$

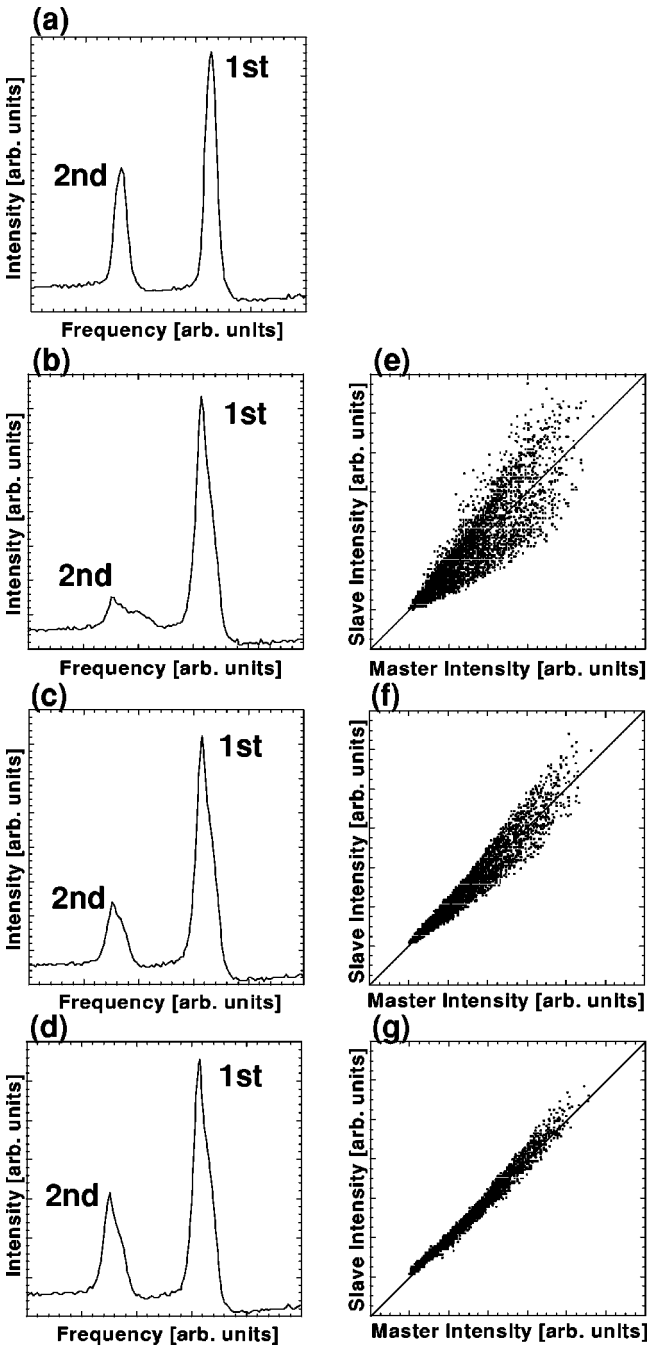

FIG. 10. Optical spectra after injection locking: (a) the master, (b),(c),(d) the slave laser outputs with two-mode oscillations, and (e),(f),(g) the corresponding correlation plots, when the temperature of the microchip crystal of the slave laser is changed.

$$\frac{dn_{0,s}}{dt} = w_{0,s}[1 + w_{p,s}\cos(2\pi\tau f_{p,s}t + \Phi_s)] - n_{0,s} - \left(n_{0,s} - \frac{n_{1,s}}{2}\right)E_s^2, \tag{4.4}$$

$$\frac{dn_{1,s}}{dt} = -n_{1,s} + (n_{0,s} - n_{1,s})E_s^2, \tag{4.5}$$

$$\frac{dE_s}{dt} = \frac{K_s}{2}\left[\left(n_{0,s} - \frac{n_{1,s}}{2}\right) - 1\right]E_s + \frac{K_s}{2}\alpha E_m \cos(\Delta\mu_{s,m}), \tag{4.6}$$

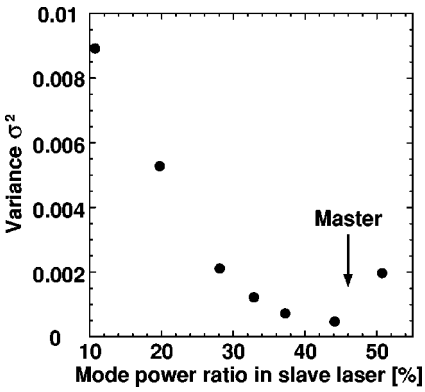

FIG. 11. Variances as a function of power spectrum ratio of the second longitudinal mode to the first mode of the slave laser after synchronization.

$$\frac{d(\Delta\mu_{s,m})}{dt} = 2\pi\tau\Delta\nu - \frac{K_s}{2}\alpha\frac{E_m}{E_s}\sin(\Delta\mu_{s,m}), \tag{4.7}$$

where n_0 and n_1 are the space averaged and the first Fourier component of the population inversion density with spatial hole burning normalized by the threshold value, respectively. E is the normalized amplitude of the lasing electrical field. $\Delta\mu_{s,m}$ is the phase difference between the master and the slave lasing field. The subscripts m, s indicate the master and slave lasers. w_0 is the optical pump parameter scaled to the laser threshold. $K = \tau/\tau_p$, where τ is the upper state lifetime and τ_p is the photon lifetime in the laser cavity. $\Delta\nu$ is the lasing frequency difference (detuning) between the two lasers. α is the coupling strength from the master to the slave laser. w_p and f_p are the pump modulation amplitude and frequency, respectively. Φ is the initial phase of pump modulation. Time is scaled by τ. We used the fourth-order Runge-Kutta method to calculate these equations.

Injection locking is required to match the optical frequencies between two lasers. The injection-locking range is defined from Eq. (4.7) as follows [41]:

$$\Delta\nu_{lock} \leqslant \frac{K_s}{4\pi\tau}\alpha\frac{E_{m,\,average}}{E_{s,\,average}}. \tag{4.8}$$

The injection-locking range is proportional to the coupling strength.

B. Numerical results

During the calculation, we set the parameter values of a Nd:YVO_4 microchip laser as follows: lasing wavelength of 1.064 μm, cavity length of 1.0 mm, refractive index of 1.9, and reflectivities of the cavity mirrors of 99.8% and 99.1% at 1.064 μm. From these values, the photon lifetime in the laser cavity is calculated to $\tau_p = 1.15$ ns. The fluorescent decay time of the upper laser level was set to $\tau = 88$ μs; thus $K = \tau/\tau_p = 7.67 \times 10^4$. When the optical pumping parameter w_0 is set at 1.7, the corresponding relaxation oscillation fre-

TABLE I. Influence of parameter mismatch on accuracy of synchronization under strong injection power (transmittance of a coupling filter of 100%). Double circles: need to be matched for accurate synchronization; circles: need to be matched for synchronization; crosses: no need to be matched.

	1-mode	2-mode
optical frequency (injection locking)	◎	○
mode power ratio	×	◎
number of modes	○	○
pumping power	×	×
relaxation oscillation frequency	×	×
injection power	×	×
pump modulation frequency	×	×
pump modulation amplitude	×	×

◎ need to be matched for accurate synchronization
○ need to be matched for synchronization
× no need to be matched

quency is 0.42 MHz. To generate chaotic oscillation in a pump modulation system, we set the pump modulation amplitude at $w_p=0.40$, the pump modulation frequency at $f_p=0.35$ MHz, and the initial phase of modulation at $\Phi_m=\Phi_s=0$.

Figure 12 shows temporal wave forms and their correlation plots for coupling strengths of $\alpha=0.03\%$ and 0.3% in MS-1 type. Here, we set $\Delta\nu=0$. As shown in Fig. 12, microchip lasers with pump modulation exhibit chaotic pulse oscillations. Synchronization is not achieved at the weak coupling strength of $\alpha=0.03\%$. When the coupling strength is increased, synchronization is achieved at the moderate coupling strength of $\alpha=0.3\%$.

In order to evaluate the accuracy of synchronization, we used the variance of the correlation plots defined by Eq. (3.1). Figure 13 shows the variances at chaos synchronization between two lasers as a function of coupling strength α in the presence of detunings between two laser frequencies at $\Delta\nu=1$ MHz (circles), 3 MHz (triangles), and 5 MHz (inverse triangles) for (a) MS-1 and (b) MS-2 ($w_{p,s}=0$). The downward arrows in Fig. 13 indicate the threshold coupling strengths for the injection-locking range $\Delta\nu_{lock}$ obtained from Eq. (4.8). We set all the parameters identical between the two lasers except the detuning of the lasing frequencies. When the optical coupling strength is increased over the threshold of injection locking, the optical frequencies are locked to each other and synchronization of chaos is achieved for both the coupling types. A clear threshold is observed and almost constant variance is maintained at coupling strengths higher than the threshold for both the coupling types. These results agree well with our experimental results shown in Fig. 4(a).

To clarify the condition to achieve chaos synchronization under the parameter mismatch between two lasers, we examine the tolerance of the deviation of laser parameters in the two lasers from perfectly identical conditions for synchronization. We set slightly different parameters in the slave laser from those in the master laser, such as the pump modulation amplitude w_p, the pump modulation frequency f_p, and the pumping power w_0. Here, we defined $\Delta w_p=w_{p,s}/w_{p,m}$, $\Delta f_p=f_{p,s}/f_{p,m}$, and $\Delta w_0=(w_{0,s}-1)/(w_{0,m}-1)$. The parameters in the master laser are fixed at $w_{p,m}$

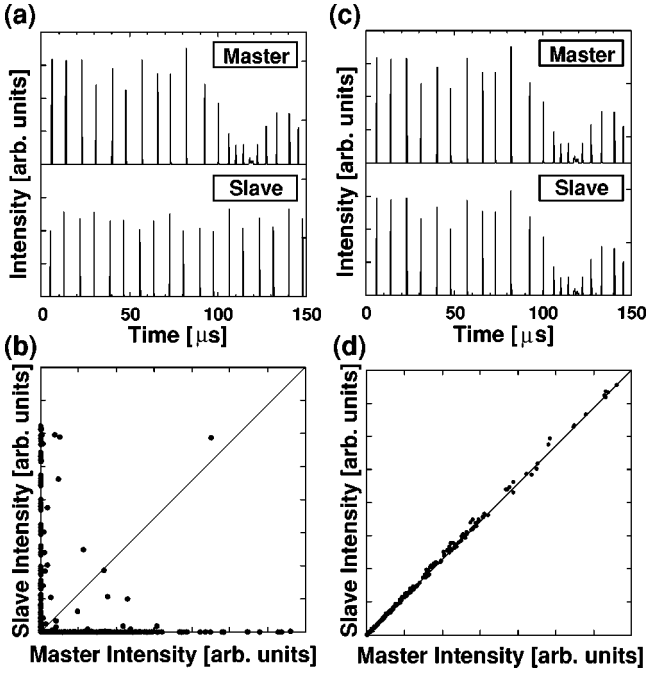

FIG. 12. Numerically obtained temporal wave forms and their correlation plots for the coupling strength $\alpha=0.03\%$ and 0.3% in MS-1 type with pump modulation at $w_p=0.40$ and $f_p=0.35$ MHz. The parameters are identical for the two lasers. (a),(b) Synchronization is not achieved at weak coupling strength $\alpha=0.03\%$. (c),(d) Synchronization is achieved at moderate coupling strength $\alpha=0.3\%$.

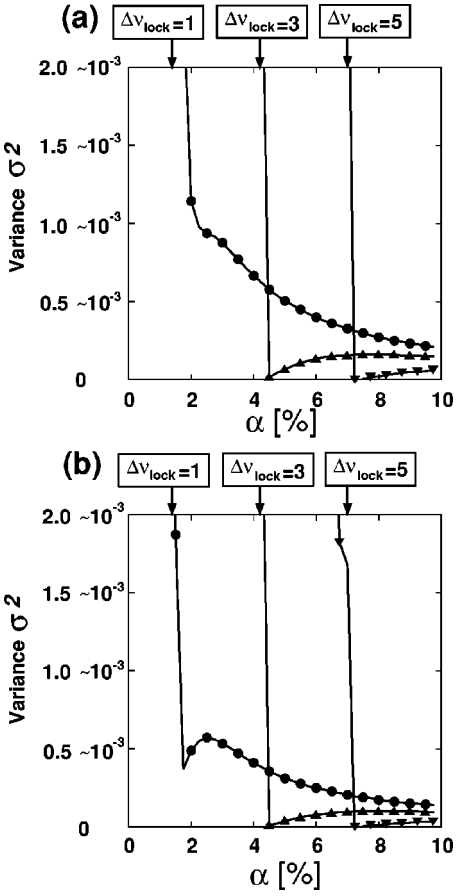

FIG. 13. Variances at chaos synchronization between two identical lasers as a function of the coupling strength α in the presence of detuning between two laser frequencies at $\Delta\nu=1$ MHz (circles), 3 MHz (triangles), and 5 MHz (inverse triangles) for (a) MS-1 and (b) MS-2 ($w_{p,s}=0$). The downward arrows indicate the thresholds of coupling strength for injection-locking range $\Delta\nu_{lock}$.

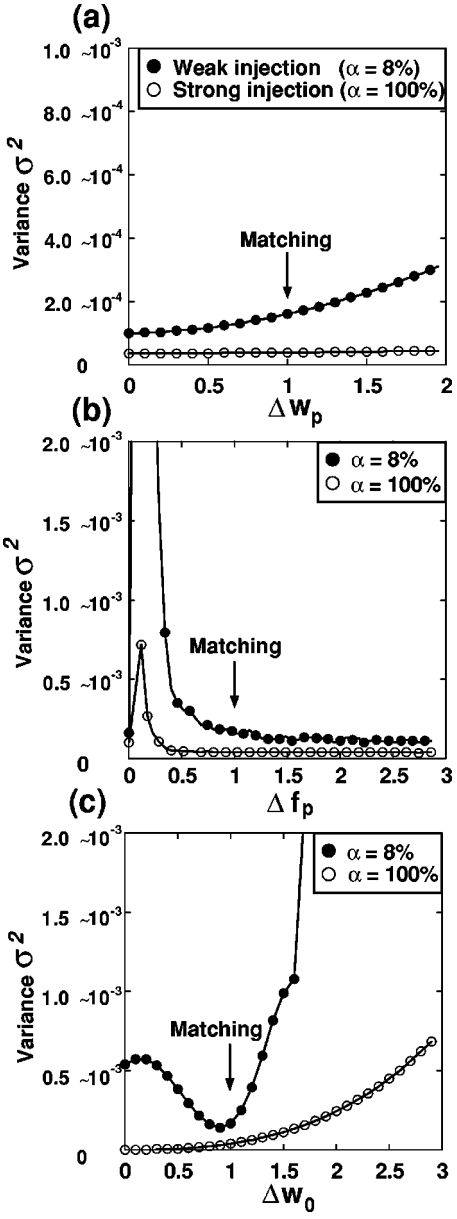

FIG. 14. Variances as functions of the parameter deviations of (a) pump modulation amplitude Δw_p, (b) pump modulation frequency Δf_p, and (c) pumping power Δw_0 for two constant coupling strengths (solid circles, $\alpha=8\%$; open circles, $\alpha=100\%$) at constant detuning of $\Delta\nu=3$ MHz in MS-1. The downward arrows indicate parameter matching between the master and slave lasers.

$=0.40$, $f_{p,m}=0.35$ MHz, and $w_{0,m}=1.7$, and the parameters in the slave laser are changed.

Figure 14 shows the variances as functions of parameter deviations of (a) the pump modulation amplitude Δw_p, (b) the pump modulation frequency Δf_p, and (c) the pumping power Δw_0 for two constant coupling strengths (solid circles, $\alpha=8\%$; open circles, $\alpha=100\%$) at a constant detuning of $\Delta\nu=3$ MHz. When Δw_p is increased at a weak coupling strength of 8%, the variance increases. The best accuracy is achieved at zero modulation amplitude, which corresponds to MS-2 type. In Fig. 14(b), the variance increases at $\Delta f_p \leqslant 0.5$ for a coupling strength of 8%, where the average amplitude of the synchronized temporal wave forms in the slave laser changes periodically in the slowly modulated slave laser, as described before. At a strong coupling strength of 100% in Figs. 14(a) and 14(b), the variance is always smaller than those at $\alpha=8\%$ and stays constant. These results agree well with those in Figs. 5(a) and 5(b).

In Fig. 14(c), when Δw_0 is increased, the variance increases dramatically for a weak coupling strength of 8%, where injection locking cannot be achieved from Eq. (4.8) because $E_{s,\,average}$ increases as Δw_0 is increased. For a strong coupling strength of 100%, synchronization is achieved in a wide parameter region. The tolerable region of parameter mismatch for synchronization is broad because of the strong injection-locking effect. These results also agree well with those in Fig. 7(b). Therefore, we have reconfirmed that the laser parameters do not need to be matched to achieve accurate synchronization.

V. CONCLUSIONS

We demonstrated experimentally and numerically the synchronization of chaos in two separate Nd:YVO_4 micro-

chip lasers with master-slave coupling schemes, and quantitatively investigated characteristics of the accuracy of synchronization in chaotic lasers under parameter mismatches. Accurate synchronization of chaos in microchip lasers reproducing a master chaos in the slave laser with an average intensity error of 2% can be maintained for over tens of hours. We conclude that the principle of chaos synchronization in lasers is based on the regeneration of the envelope of the chaotic master laser in the slave cavity through the mechanism of injection locking. The condition to achieve accurate synchronization of chaos is almost equivalent to the injection-locking range. Modulation in the slave laser reduces the accuracy of the synchronization at weak injection levels, whereas the accuracy of synchronization is always maintained at strong injection levels even when the parameter mismatch between the two lasers is changed. In two-mode lasers, chaos synchronization requires locking all the corresponding longitudinal modes to each other between the two lasers. The power spectrum ratio of longitudinal modes needs to be matched for accurate synchronization, which is a more severe condition for imitating the original chaos with unauthorized laser cavities.

ACKNOWLEDGMENTS

We gratefully acknowledge R. Roy, J. M. Liu, A. Gavrielides, V. Kovanis, K. A. Shore, S. Sivaprakasam, L. Larger, G. D. VanWiggeren, K. Otsuka, T. Taira, J. Ohtsubo, P. Davis, Y. Liu, I. Fischer, A. Murakami, Y. Takiguchi, H. Fujino, F. Kuwashima, and H. Iwasawa for helpful discussions. This work was supported by the Foundation ''Hattori-Hokokai.''

[1] L. M. Pecora and T. L. Carroll, Phys. Rev. Lett. **64**, 821 (1990).
[2] K. M. Cuomo and A. V. Oppenheim, Phys. Rev. Lett. **71**, 65 (1993).
[3] G. D. VanWiggeren and R. Roy, Science **279**, 1198 (1998); G. D. VanWiggeren and R. Roy, Phys. Rev. Lett. **81**, 3547 (1998); G. D. VanWiggeren and R. Roy, Int. J. Bifurcation Chaos Appl. Sci. Eng. **9**, 2129 (1999).
[4] J.-P. Goedgebuer, L. Larger, and H. Porte, Phys. Rev. Lett. **80**, 2249 (1998); L. Larger, J.-P. Goedgebuer, and F. Delorme, Phys. Rev. E **57**, 6618 (1998).
[5] S. Sivaprakasam and K. A. Shore, Opt. Lett. **24**, 1200 (1999); S. Sivaprakasam and K. A. Shore, IEEE J. Quantum Electron **36**, 35 (2000).
[6] A. Uchida, T. Ogawa, and F. Kannari, Jpn. J. Appl. Phys., Part 2, **37**, L730 (1998).
[7] H. G. Winful and L. Rahman, Phys. Rev. Lett. **65**, 1575 (1990).
[8] V. Annovazzi-Lodi, S. Donati, and A. Scire, IEEE J. Quantum Electron. **33**, 1449 (1997).
[9] P. M. Alsing, A. Gavrielides, V. Kovanis, R. Roy, and K. S. Thornburg, Jr., Phys. Rev. E **56**, 6302 (1997).
[10] A. P. Napartovich and A. G. Sukharev, Quantum Electron. **28**, 81 (1998).
[11] P. Colet and R. Roy, Opt. Lett. **19**, 2056 (1994).
[12] V. Ahlers, U. Parlitz, and W. Lauterborn, Phys. Rev. E **58**, 7208 (1998).
[13] C. L. Pando, Phys. Rev. E **57**, 2725 (1998).
[14] P. S. Spencer, C. R. Mirasso, and K. A. Shore, IEEE J. Quantum Electron. **34**, 1673 (1998).
[15] P. S. Spencer and C. R. Mirasso, IEEE J. Quantum Electron. **35**, 803 (1999).
[16] C. T. Lewis, H. D. I. Abarbanel, M. B. Kennel, M. Buhl, and L. Illing (unpublished).
[17] H. F. Chen and J. M. Liu, IEEE J. Quantum Electron. **36**, 27 (2000).
[18] L. G. Luo and P. L. Chu, J. Opt. Soc. Am. B **15**, 2524 (1998).
[19] C. R. Mirasso, P. Colet, and P. G.- Fernandez, IEEE Photonics Technol. Lett. **8**, 299 (1996).
[20] V. Annovazzi-Lodi, S. Donati, and A. Scire, IEEE J. Quantum Electron. **32**, 953 (1996).
[21] A. Sanchez-Diaz, C. R. Mirasso, P. Colet, and P. Garcia-Fernandez, IEEE J. Quantum Electron. **35**, 292 (1999).
[22] J. K. White and J. V. Moloney, Phys. Rev. A **59**, 2422 (1999).
[23] C. L. Pando, Phys. Lett. A **223**, 369 (1996).
[24] L. Rahman, G. Li, and F. Tian, Opt. Commun. **138**, 91 (1997).
[25] R. Kuske and T. Erneux, Opt. Commun. **139**, 125 (1997).
[26] M. Sauer and F. Kaiser, Phys. Lett. A **243**, 38 (1998).
[27] T. Sugawara, M. Tachikawa, T. Tsukamoto, and T. Shimizu, Phys. Rev. Lett. **72**, 3502 (1994).
[28] D. Y. Tang, R. Dykstra, M. W. Hamilton, and N. R. Heckenberg, Phys. Rev. E **57**, 5247 (1998); D. Y. Tang, R. Dykstra, M. W. Hamilton, and N. R. Heckenberg, Chaos **8**, 697 (1998).
[29] S. Sivaprakasam and K. A. Shore, Opt. Lett. **24**, 466 (1999).
[30] R. Roy and K. S. Thornburg, Jr., Phys. Rev. Lett. **72**, 2009 (1994).
[31] J. R. Terry, K. S. Thornburg, Jr., D. J. DeShazer, G. D. VanWiggeren, S. Zhu, P. Ashwin, and R. Roy, Phys. Rev. E **59**, 4036 (1999).
[32] Y. Liu, P. C. de Oliveira, M. B. Danailov, and J. R. Rios Leite, Phys. Rev. A **50**, 3464 (1994).
[33] D. Y. Tang, R. Dykstra, and N. R. Heckenberg, Phys. Rev. A **54**, 5317 (1996).
[34] A. Hohl, A. Gavrielides, T. Erneux, and V. Kovanis, Phys. Rev. Lett. **78**, 4745 (1997); Phys. Rev. A **59**, 3941 (1999).
[35] T. Tsukamoto, M. Tachikawa, T. Hirano, T. Kuga, and T. Shimizu, Phys. Rev. E **54**, 4476 (1996).
[36] Y. Liu and P. Davis, Opt. Lett. **25**, 475 (2000).
[37] Y. Takiguchi, H. Fujino, and J. Ohtsubo, Opt. Lett. **24**, 1570 (1999).
[38] A. Uchida, M. Shinozuka, T. Ogawa, and F. Kannari, Opt. Lett. **24**, 890 (1999).
[39] H. Fujisaka and T. Yamada, Prog. Theor. Phys. **69**, 32 (1984).
[40] K. Pyragas, Phys. Lett. A **181**, 203 (1993).
[41] A. E. Siegman, *Lasers* (University Science Books, Mill Valley, CA, 1986).
[42] K. Otsuka, IEEE J. Quantum Electron. **QE-15**, 655 (1979).
[43] K. Otsuka, Jpn. J. Appl. Phys., Part 2, **31**, L1546 (1992).
[44] A. Uchida, T. Sato, and F. Kannari, Opt. Lett. **23**, 460 (1998).
[45] A. Uchida, T. Sato, T. Ogawa, and F. Kannari, Phys. Rev. E **58**, 7249 (1998).

[46] T. Taira, A. Mukai, Y. Nozawa, and T. Kobayashi, Opt. Lett. **16**, 1955 (1991).

[47] K. Kovanis, A. Gavrielides, T. B. Simpson, and J. M. Liu, Appl. Phys. Lett. **67**, 2780 (1995).

[48] E. G. Lariontsev, I. Zolotoverkh, P. Besnard, and G. M. Stéphan, Eur. Phys. J. D **5**, 107 (1999).

[49] C. L. Tang, H. Statz, and G. deMars, J. Appl. Phys. **34**, 2289 (1963).